

A Palmprint-Based Identification System using Radon Transform

Shimaa M. Al-seddek, Hassan H. Soliman, Muhammad S. Morsy , Sherif S. Kishk

ECE Department, Faculty of Engineering, Mansoura University,

Mansoura – Egypt

sh_sediek@yahoo.com, hhsoliman@yahoo.com, drmmorsy@yahoo.com, shkishk@mans.edu.eg

Abstract

This paper proposes a palmprint-based identification system using Radon transform. Palmprint is a reliable identification method because the print patterns are unique even in the monozygotic twins, has permanent ridge structure, has fixed line structure, user friendliness, low cost capturing devices, and low resolution imaging. The proposed system is applied to CASIA database. Radon transform is used for extracting the features because it can be used in palm lines detection with high precision and efficiency. Live and enrolled palmprint are matched using Euclidean distance for verification. This system can achieve Equal Error Rate (EER) of 0.47% and Genuine Acceptance Rate (GAR) of 99.56%. The results of this study showed that the proposed system achieves higher verification accuracy than other palmprint identification systems.

Keywords: *Identification, Biometrics, CASIA, Palmprint, Radon Transform, Euclidean Distance.*

1. Introduction

Personal identification systems using biometric features have been widely used in critical security applications such as banking, access control and crime investigation. Examples of these biometric features include Fingerprint, Iris, Face, Hand geometry, Palmprint, etc. Fingerprint and Face recognition are the most widely studied biometrics. The reliability of Face biometrics has been hampered by the problems caused by pose, expressions and illumination. For decades now, Fingerprint is the most effective identification system. However, it also has some limitations as different groups of users such as elderly people and manual workers fail to deliver good quality fingerprint images [1]. In addition, noise caused by multiple fingerprints on the device sensor negatively affects the efficiency of the identification system. Iris recognition is another reliable method, but its acquisition device is relatively expensive and it is not very convenient to collect [2].

Of all the above-mentioned systems, the Palmprint-based identification system has been intensively developed because of its advantages over other features. Compared to other biometric systems, palmprint has many advantages such as high accuracy, user friendliness and low resolution imaging that can be employed in palmprint recognition that is based on creases and palm lines, making it possible to perform well in real time pre-processing and feature extraction steps. It has a large area for extracting features and is more resistant to injuries and dirt compared to fingerprint. In these cases, the distinguishable features rely on palm lines and texture patterns [3]. These specific line features are extracted after applying effective pre-processing filters to enhance the Region of Interest (ROI) of palmprint images.

Recently, several methods have been proposed for palmprint identification. The methods presented in [4-7] could extract dominant line features but may miss some fine structural information of palmprint [8]. The wavelet coefficients could represent discriminating information for palmprint, but it is too slow for some real time applications [9, 10]. There are methods that have achieved high levels of speed and accuracy such as code line orientation [11-13] where palm lines are viewed as negative lines. One such method is the competitive code (CompCode) [11]. This method, which applies six real parts of Gabor filters to each palmprint ROI for generating the corresponding orientation map and is thus very complex and too slow for real-time application especially on slow mobile platforms. Wu et al. [12] used a similar idea but used four self-devised directional templates to shorten the feature extraction time. In this case the extracted code was called palmprint orientation code (POC). Jia et al. [13] extracted orientation information using modified finite Radon transform (MFRAT) proposed in robust line orientation code (RLOC) to avoid “warp around” [2].

This paper proposes a system to extract specific information about the rotation and scaling invariant features of palmprint images using Radon transform. In this system the Euclidean distance is used to produce high identification accuracy in image matching. The paper is divided into the following sections; Section 2 discusses data acquisition of palmprint images while section 3 describes the proposed system, the Radon transform which has been used to extract the features of the palmprint and the matching technique that is used to identify the palmprint images. Experimental results on CASIA database and robustness of the system are presented in section 4. The conclusion is presented in the last section.

2. Data Acquisition

In the proposed system data were collected from CASIA which is a palmprint database containing 5502 palmprints captured from 312 subjects [14]. To the best of our knowledge, this database is the largest publicly available database in terms of the number of subjects. For each subject, the left and right images have been captured. All the palmprint images are 8 bit gray level JPEG files. These palmprint images have been captured by a self-development palmprint recognition device which imposes less physical constraints on the user's palm leading to more obvious palm movements, distortions, and blurring in the captured palmprint images [15]. There are no pegs to restrict the postures and positions of the palms during the data collection, which allowed a high degree of freedom. Subjects were required to put their palms onto the device and lay them on a uniform-colored background. The device supplies an evenly distributed illumination and captures palmprint images using a CMOS camera fixed on the top of the device. Some of the palmprint images captured by the CASIA palmprint recognition device are shown in figure 1. CASIA database was selected because its images were captured using web cameras, which means low resolution images and low cost capturing device. Thus, the image quality was not as good as other palmprint database images such as PolyU. Compared with other databases, CASIA has a large number of palm images for which it may be very difficult to obtain high performance rates by using traditional palmprint-based identification systems [16, 17, 18].

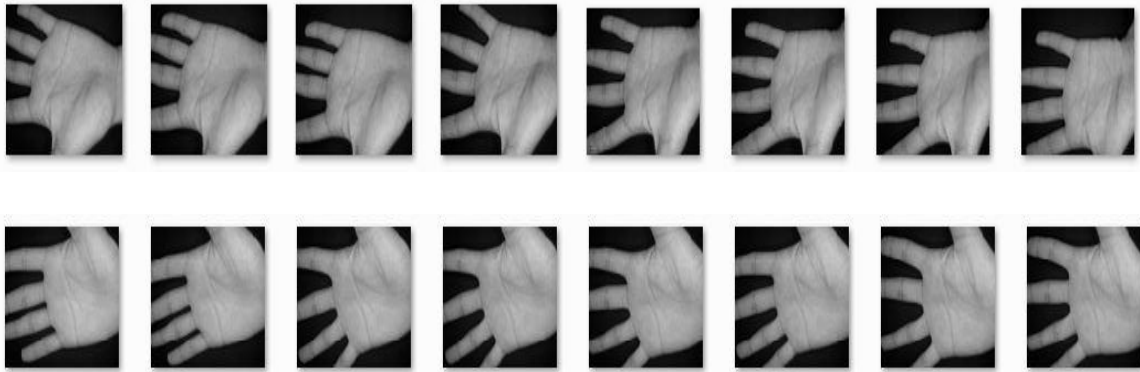


Figure 1: Sample of One person from CASIA Palmprint Database.

3. The Proposed System

The proposed palmprint-based identification system starts with acquiring the input image of the hand using a low- cost device. Eight different variations of one hand palmprint captured images are used. These images are different in both rotation and scaling position. The acquired hand image is pre-processed to be enhanced before palmprint ROI is extracted. In the next step, effective filters are applied to the extracted ROI to improve the palm lines which are to be extracted as features using Radon transform. Then the features of live palmprint are matched with the corresponding palmprint enrolled in the database. The matching decision is done based on a threshold value that can be defined as the distance between the test image and the database images. Threshold values are recorded as Error Vector (EV) using distance formula and then the average of the EV is considered as the threshold value for recognition declaration to identify persons accurately [19]. The proposed palmprint identification system has been depicted in figure 2 below:

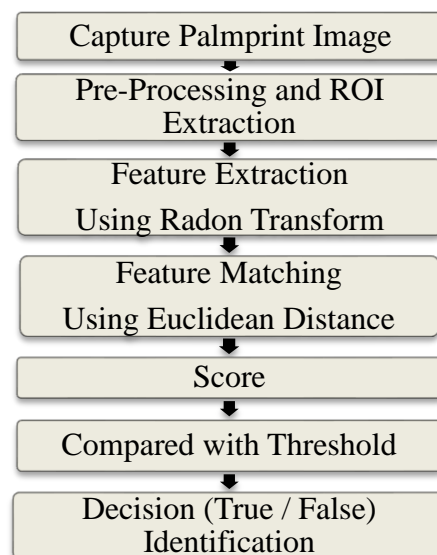


Figure 2: Flowchart of Palmprint Algorithm

3.1 Pre-processing and Extracting the Region of Interest

At this stage, the Region of Interest (ROI) is extracted from the palmprint image. Before the ROI is extracted from the CASIA palmprints, the palmprint images are resized to 380×284 pixels. After that the extracted ROI is binarized using best fixed threshold value. Then the isolated pixels of morphological filters were applied for enhancing the resultant image. The boundary tracking algorithm [20] is used to obtain the boundary of the binarized palmprint images. The next step, using a curvature maxima finding algorithm [21] to allocate the maximum curvature points P1 and P2 that laying between the fingers as shown in figure 3. Next, P1 and P2 are connected by line, L1, then L2 drawn starting with P3, the middle point of L1, and ending at P4 the center point of the extracted square ROI S (150×150 pixels).

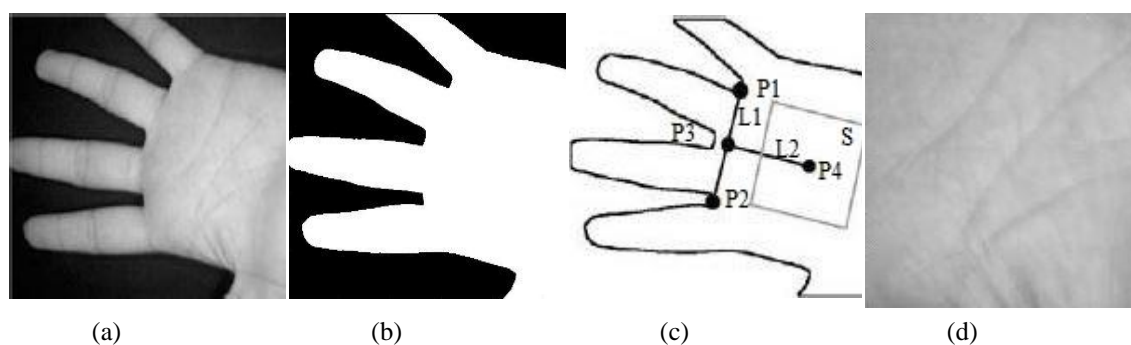


Figure 3: A CASIA palmprint and the corresponding ROI extraction.

CASIA palmprint images have a uniform reflection from the relatively curvature surface with uniform brightness. Pre-processing filters are applied to the extracted ROI of the palmprint images. These filters include Sobel filter and Canny filter. They are used to obtain good enhanced images for extracting the palm lines.

In this paper, using these filters improved the ability of Radon transform in detecting the palm lines. Figure 4 shows the filters results.

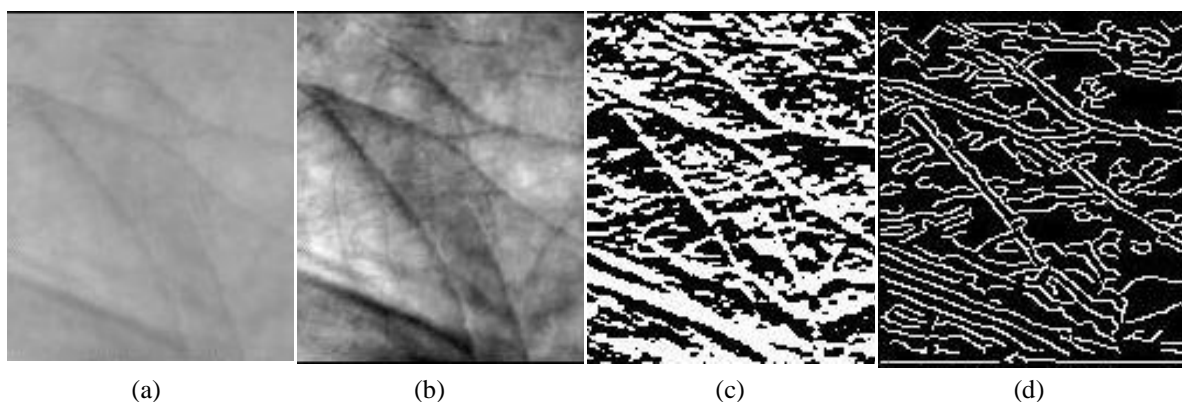


Figure 4: Filters applied on the extracted palmprint ROI, (a) The ROI, (b) After histogram Equalization, (c) After Sobel filter and (d) After Canny filter.

3.2 Feature Extraction Using Radon Transform

Radon transform can be used for line detection. In this paper, palm lines are detected from the ROI as features using Radon transform. The proposed method is based on applying the Radon transform on palmprint image $f(x, y)$ and then computing the projection of the image. The resulting projection is the sum of the intensities of pixels in each direction, i.e. a line integral. The result is a new image $R(\rho, \theta)$ that can be written mathematically by defining

$$\rho = x \cos\theta + y \sin\theta \tag{1}$$

After which the Radon transform can be written as

$$R(\rho, \theta) = \iint_{-\infty}^{\infty} f(x, y) \delta(\rho - x \cos\theta - y \sin\theta) dx dy \tag{2}$$

Where (x, y) denote the spatial coordinates and ρ denotes the radial (perpendicular) distance from the coordinate origin to the line with angle (θ) [22]. The relations of these parameters with the spatial coordinate system is shown in figure 5.

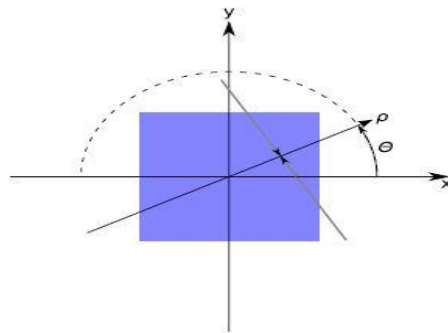


Figure 5: For each angle θ and each distance ρ the intensity of the matter a ray Perpendicular to the ρ axis crosses are summed up at $R(\rho, \theta)$ [23].

Radon Transform possesses some important properties. The most important properties are Linearity, Shifting and Rotation.

Thus, Radon transform is applied to the enhanced palmprint ROI for extracting the palmprint features. After that line integrals are computed at different directions ranging from 0-179 degree. These features vectors of the palmprint image were used as feature map. The results are shown in figure 6.

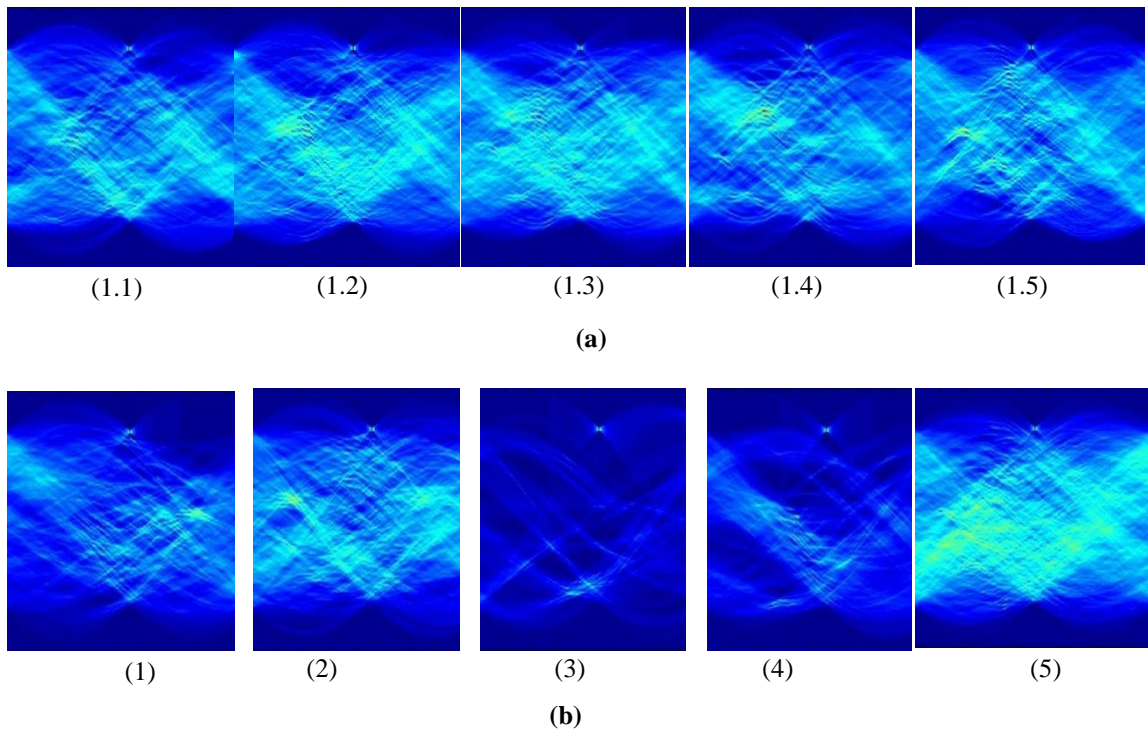


Figure 6: Radon transform of ROI palmprint images, (a) Illustrate resulting Radon transform of 5 different captures of the same person's left hand, (b) Illustrate resulting Radon transform of 5 different people's left hands.

3.3 Matching

In this paper, in order to identify a person after his palmprint has been captured, the Radon transform for the enrolled palmprint should be matched with the Radon transform of the corresponding live palmprint using the Euclidean distance method.

Other orientation coding-based palmprint verification methods, such as competitive code, palmprint orientation code and robust line orientation code have fast matching speeds. Orientation code methods use two types of distance measuring methods, SUM_XOR (angular distance) and OR_XOR (Hamming distance). The extracted method called CompCode use the angular distance method to measure the dissimilarity between two features vectors. It can be defined as in equation 3.

$$D_{SUM_XOR} = \frac{\sum_{y=1}^M \sum_{x=1}^N \sum_i^3 P_i^b(x,y) \otimes Q_i^b(x,y)}{3 * M * N} \quad (3)$$

Where P and Q are two CompCode features, P_i^b or Q_i^b is the i^{th} bit plane of P or Q and \otimes is a bitwise exclusive OR (XOR).

The extracting feature method called RLOC use Hamming distance. For each pixel, the angular distance is the sum of the three XOR resulting on each bit. Thus the angular distance can be called the SUM_XOR distance that defined as in equation 4 [3].

$$D_{Hamming}(P, Q) = \frac{H(P, Q)}{M * N} \tag{4}$$

Where $H(P, Q)$ is defined as the number of pixels at which the values of P and Q are different.

In this paper, The Euclidean distance is calculated between two images in the Radon space. If the metric coefficients depend properly on the pixel distances, the obtained Euclidean distance is sensitive to small deformation. Let p_i, p_j are the two matched images and $i, j=1, 2, \dots, M, N$, be pixels, where M, N are the total number of pixels in the two image respectively. The pixels distance written as $|p_i - p_j|$ are the distance between p_i and p_j on the image lattice. Pixels or picture elements (pel) are defined as a single point image which are addressable as small screen elements. Each pixel can be controlled and represented using a dot or a square with its own address. The address corresponds to its coordinates with a two dimensional grid. For example, p_i is at location (k, l) and p_j is at (k', l') , thus $|p_i - p_j|$ may be $(k - k')^2 + (l - l')^2$ [24]. Then if the resulting value from the Euclidean distance formula is equal or less than the selected threshold value, the two matched images are similar. This gives an indication that the person can be identified correctly. On the other hand, if the resulting value from the Euclidean distance formula is more than the threshold value, the person cannot be identified correctly.

4. Experimental Results

The system proposed in this paper is tested on CASIA palmprint database. In this experiment, a total of 640 images were taken for 10 subjects. There were 8 images of the same hand which have variations on scaling, rotation and shifting position. The extracted ROI contain more discriminating information about palmprint images as it is rich in lines. The output of Radon transform is used to detect palm lines as features map representation. The experimental results obtained are shown in figures 7 and 8.

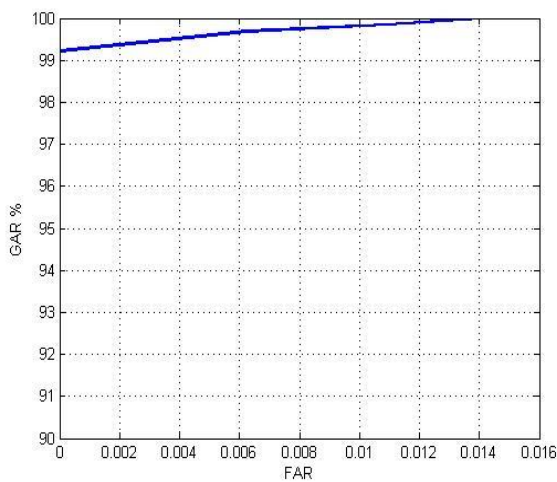


Figure 7: ROC curve

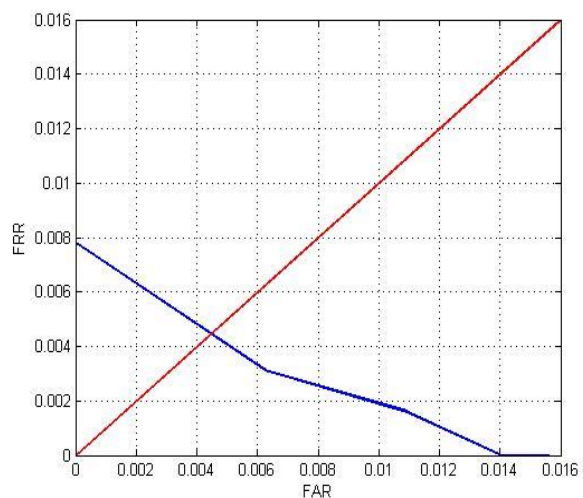


Figure 8: EER curve

Where figure 5, the ROC curve, shows that the model achieved a high identification accuracy rate 99.56%. The x, y axis are defined as False Acceptance Rate (FAR) and Genuine Acceptance Rate (GAR) respectively, where FAR is the percentage of queries that are wrongly identified as other subject , the ratio of the number of false acceptances to the number of identification attempts, and it is given in equation 5 [25].

$$FAR = \frac{\text{No. of unauthorized test images accepted}}{\text{Total no. of identification attempts}} \quad (5)$$

GAR is the percentage of queries that are correctly identified. It measures the percentage of matching rate regardless of the False Rejection Rate (FRR), where it is given in equation 6 [25].

$$GAR = \frac{\text{No. of test images matches correctly}}{\text{Total no. of identification attempts}} \quad (6)$$

FRR is the percentage of queries which are identified as “no match”, the ratio of the number of false rejection to the number of identification attempts, and it is given in equation 7 [25].

$$FRR = \frac{\text{No. of authorized person rejected by the system}}{\text{Total no. of identification attempts}} \quad (7)$$

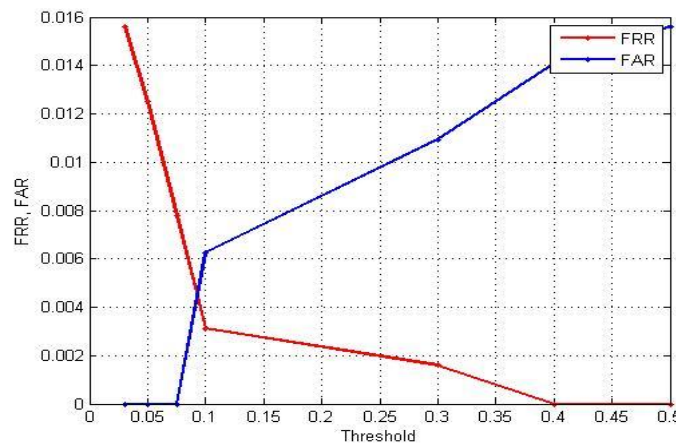


Figure 9: EER VS Threshold

ERR, the rate at which both accept and reject errors are equal, is illustrated in figure 8 and 9. The system with the least ERR is the most accurate [19]. As known, EER gives an indication of the systems performance. The proposed system showed high identification accuracy 99.56% and low equal error rate 0.47% by using Euclidean distance as a measure distance for classifications in the matching stage. The time performance of the proposed system is illustrated again in, table 1 which shows the execution time of the proposed system. The proposed system has been implemented using MATLAB 2012b on an Intel core i3, CPU power 2.3 GHz, 3G RAM, and windows 7 operating system.

Table 1: Illustrate the execution time during the proposed model.

Processing stages	Execution time (ms)
Pre-processing	1200
Feature extraction	150
Matching	2
Decision	6

The accuracy and robustness of the proposed system compared to other best known palmprint identification systems shown in table 2.

Table 2: Comparison of error rates of different palmprint verification methods on the CASIA palmprint database.

Method	EER%	GAR %
Proposed system	0.47	99.56
CompCode [11]	0.58	97.60
RLOC [13]	0.81	96.31
OrdiCode [15]	0.84	96.80
2D SAX [16]	0.9	99.90
CompFeat [26]	3.2	97.2

Table 2 lists the values of GAR and the values of EER of the proposed system, competitive code (CompCode), RLOC, ordinal code (OrdiCode), 2D-SAX and Compound Features (CompFeat). We use GAR to denote the genuine acceptance rate when EER equals 0.47%. Compared with these methods, the proposed system achieves the lowest EER value. The GAR of the proposed system is 99.56, which is slightly lower than that of 2D-SAX and is higher than that of competitive code, ordinal code, RLOC and CompFeat. Thus, this paper proposes a more accurate and effective palmprint based-identification system.

5. Conclusion

This paper presents a Radon transform based palmprint identification system, CASIA is used as Palmprint images Database. Radon transform is used as a feature extraction technique as it operated well in palm lines detection. The proposed system, compared to the other best known systems, has better performance. It can also be used in real time security applications as it takes 150 ms in the feature extraction process. This system also has the advantage of fast matching speed by using Euclidean distance.

References

- [1] A. Mostayed, M. Kabirt, S. Khan and M. Mazumder “Biometric Authentication from Low Resolution Hand Images Using Radon Transform”, In ICCIT PP587592, 2009.
- [2] Z. Guo, W. Zuo, L. Zhang and D. Zhang, “A unified distance measurement for orientation coding in palmprint verification”, In Neurocomputing 73, ScienceDirect, pp 944–950, 2010.
- [3] J. Chaudhari¹, P. M. Patil² and Y. P. Kosta³, ” Features extraction using histogram of Radon transform for palmprint matching ”, In IJAET, pp 2231-1963, 2012.
- [4] C.-C. Han, H.-L. Cheng, C.-L. Lin and K.-C. Fan, “Personal authentication using palm- print features “, Pattern Recognition 36, pp 371–381, and 2003.
- [5] C.-L. Lin, T.C. Chung and K.-C. Fan, “Palmprint verification using hierarchical decomposition”, Pattern Recognition 38, pp 2639–2652, 2005.
- [6] X. Wu, D. Zhang and K. Wang, “Palm line extraction and matching for personal authentication”, IEEE Transactions on System, Man, and Cybernetics, Part A 36, pp. 978–987, 2006.
- [7] D.-S. Huang, W. Jia and D. Zhang, “Palmprint verification based on principal lines”, Pattern Recognition, pp. 1316–1328, 2008.
- [8] D. Zhang, W. Kong, J. You and M. Wong,” Online palmprint identification”, IEEE Transactions on Pattern Analysis and Machine Intelligence 25, pp. 1041–1050, 2003.
- [9] L. Zhang and D. Zhang, “Characterization of palmprint by wavelet signatures via directional context Modeling”, IEEE Transactions on System, Man, and Cybernetic, Part B 34, pp 1335–1347, 2004.
- [10] G. Y. Chen, T. D. Bui and A. Krzyzak, “Palmprint classification using dual-tree complex wavelets”, in: International Conference on Image Processing, pp. 2645–2648, 2006.
- [11] Kong and D. Zhang, “Competitive coding scheme for palmprint verification”, in: International Conference on Pattern Recognition, pp. 520–523, 2004.
- [12] X. Wu, K. Wang and D. Zhang, “Palmprint authentication based on orientation code matching”, in: Audio- and Video-Based Biometric Person Authentication, pp. 555–562, 2005.
- [13] W. Jia, D.-S. Huang, D. Zhang, “Palmprint verification based on robust line orientation code”, Pattern Recognition 41, pp 1504–1513, 2008.
- [14] CASIA Palmprint Database, <http://www.cbsr.ia.ac.cn/english/Palmprint%20Databases.asp>.
- [15] Z. Sun, T. Tan, Y. Wang, and S. Z. Li, ” Ordinal palmprint representation for personal identification”, Proceedings of IEEE International Conference on CVPR 2005, pages 279–284, Orlando, USA, 2005.
- [16] J. Chen, Y. Moon, Ming-Fai and G. Su, “Palmprint authentication using a symbolic representation of images “Image and Vision Computing 28, ScienceDirect, pp. 343–351, 2010.

- [17] J. Kour¹, S. Vashishtha², N. Mishra³, G. Dwivedi⁴ and P. Arora, “Palmprint Recognition System”, In IJIRSET, pp. 1006-1009, 2013.
- [18] W. Zuo, Z. Lin, and Z.Guo, D.Zhang, “The Multiscale Competitive Code Via Sparse Representation for Palmprint Verification” proceedings of IEEE, pp. 2265-2272, 2010.
- [19] J. P. GEORGE and K. B. RAJA, “DEVELOPMENT OF EFFICIENT BIOMETRIC RECOGNITION ALGORITHMS BASED ON FINGERPRINT AND FACE”, A thesis for the degree of doctor of philosophy in computer science, pp 1-158, Christ University, Bangalore – 560029 march, 2012.
- [20] A.Rosenfeild and A.C. Kak, “Digital Picture Processing”, Academic Press, San Diego, 1982.
- [21] M.H Han and D.Jang, “The use of maximum curvature points for the recognition of partially occluded objects”, Pattern Recognition 23, pp 21-23, 1990.
- [22] Badrinath G. S., N. Kachhi and P. Gupta,” Palmprint based Verification System Robust to Occlusion using Low-order Zernike Moments of Sub-images”, In BMVC, Pages 1-11, 2009.
- [23] C. Høilund,”The Radon Transform”, Aalborg, November 12, 2007.
- [24] L. Wang, Y. Zhang and J. Feng, “On the Euclidean Distance of Images”, Beijing, 100871, China, 2004.
- [25] F. Yue, B. Li, M. Yu, and J. Wang, “Hashing Based Fast Palmprint Identification for Large-Scale Databases”, proceedings of IEEE Transaction on Information Forensics and Security, pp 769-778, Vol. 8, No. 5, May 2013.
- [26] N. L. Manasa, A. Govardhan, Ch. Sathanarayana, “ Hybrid Approach for Palmprint Recognition Using Compound Features” , Springer Link, pp 16-27, 2013.